Exact Perturbed Unsteady Boundary Layers

S.P. Farthing

Econologica, N. Saanich BC Canada

Abstract: The time diffusive boundary layer from rest for Taylor series uniform outer flow is constructed by integration of the complementary error function of the diffusive similarity variable . The same erfc solution is also easily "Stokes" transformed to solve harmonic outer flow from rest.

If the outer flow vector varies weakly along the boundary, the perturbation pressure gradient accelerates the slowest fluid nearest the wall the most to disproportionately vary the shear stress. So centripetal acceleration causes secondary crossflow inside the boundary layer with strong wall shear towards the center of curvature. But longitudinal acceleration also implies an inflow towards the wall which thins the outer boundary layer with a weak further increase of the wall shear, but the strongest perturbation steady streaming.

Simple new particular solutions for these two perturbations are easily constructed in terms of products of integrals and derivatives of any *primary diffusive solution. For an outer flow as a series in the square root of time, all homogeneous time coefficients remain just iterated error functions. Each systolic pulse in the aortic arch was considered as a Taylor series flow from rest to calculate the wall shear vectors.*

When the outer flow oscillates forever more, its primary diffusive boundary layer asymptotes to the Stokes oscillatory exponential decay with distance from the wall. The particular perturbations are exactly evaluated and also confined near the wall but with mean slip. The mean slip homogenous perturbations diffuse outside the Stokes layer into steady streaming as complementary error functions with inverse time correction functions. Extended Taylor series computations provide more detail of the perturbation transients.

Keywords: Heat Diffusion Equation, Secondary Flow; Steady Streaming,; Stokes

I. Introduction

A theoretical study [1] was undertaken of the boundary layer in the aortic arch with a view to possibly explaining the patchy occurrence of atherosclerotic lesions on the arch walls, for instance due to variation blood particle motion near the wall[2]. Experimental study of the boundary layer is complicated by the flexibility of the aortic wall and the difficulty of *in vivo* examination, requiring the sacrifice of large animals such as horses.

The local diffusive boundary layer was perturbed for pressure gradients and inflow due to the helical curvature of the aortic arch and the stream wise variation of that curvature' strength and plane. The maximum bend is tight and it was not necessary to resort to the inappropriate small curvature approximation commonly used. In fact the numerical results were quite different than the low curvature ones, with secondary flow on the inside of the bend much intensified by the stronger potential vortex core flow there. This indicated the secondary flow would focus into a jet normal to the wall at the very inside of the bend. The jet separates the boundary layer and injects vorticity into the flow as a whole. This intrusion of the boundary layer into the bulk flow is seen in the pulsed Doppler ultrasound profiles of Peronneau [3]. Downstream in a light coil, this core vorticity would eventually transform the flow into the high Dean number steady flow of greater axial velocity near the outside of the bend.

Some correlations were found between wall shear variations and the patterns of disease which is actually different from that of dye uptake and other experimental patterns. Unfortunately no absolutely compelling matches were found and the entire physiological localisation patterns and possible mechanisms need closer scrutiny rather than further flow studies.

During this work simple ways were found to construct homogeneous solutions for the diffusion (heat) equation and first order solutions for fluid spatial acceleration perturbations of it. These might also be adapted to solution and perturbation of other linear pde's. Here they will be presented for the generalised fluid dynamic problem of perturbing starting and oscillatory boundary layers for spatial acceleration of the coreflow.
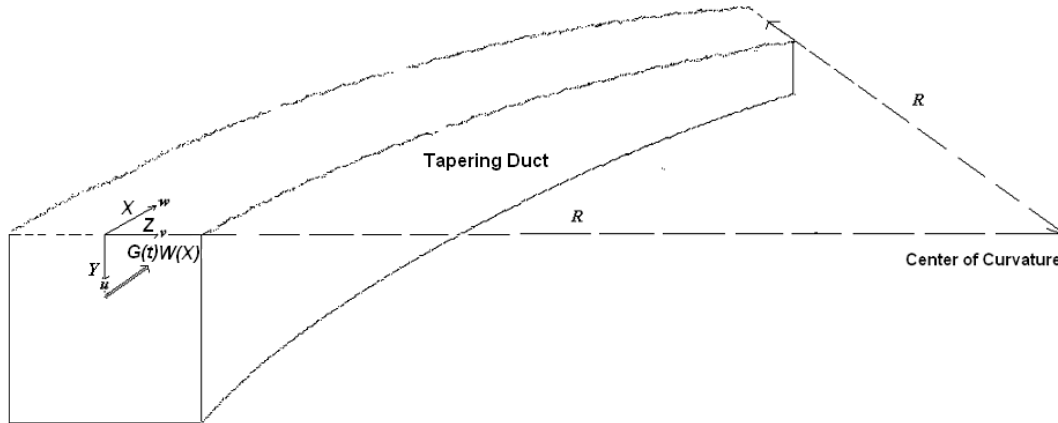
Figure 1 Illustrative Geometry

II.   Perturbed Diffusive Boundary layer Equations

As a *simple* illustrative case consider the inviscid incompressible streamline velocity $G(\tau)W(X)$ parallel to and small distance Y below the centerline of the top wall of a slightly tapered square duct, as in Figure 1. Here $G(\tau)$ is a non-dimensional O(1) pulsatory/oscillatory time factor starting at time $\tau=0$. Then the axial X gradient of pressure p due to temporal and advective accelerations resp. is the inviscid

$$\mathbf{d}_X p = -\rho \, (W\mathbf{d}_\tau G + G^2 W\mathbf{d}_X W) \quad (1)$$

with ρ the density. With ν the kinematic viscosity, the 2D boundary layer equation for the centerline velocity w at small distance Y below the top wall is

$$\mathbf{d}_\tau w + w\mathbf{d}_x w + u\mathbf{d}_Y w = -\mathbf{d}_x p/\rho + \nu \mathbf{d}^2{}_Y w \quad (2) \quad \text{where } \mathbf{d}_Y u + \mathbf{d}_X w = 0 \quad (3)$$

$w=0$ at $Y=\tau=0$ and w tends to GW as Y tends to ∞.

Let $t= \tau /T$, T a characteristic time such as the angular period of a harmonic G, and let $y=Y/\sqrt{\nu T}$, the characteristic diffusion distance scale in time T

Then $\mathbf{d}_\tau - \nu \mathbf{d}^2{}_Y$ becomes D/T where $D= \mathbf{d}_t - \mathbf{d}^2{}_y$ is the Diffusion operator

When the $W\mathbf{d}_\tau G$ dominates $G^2 W\mathbf{d}_X W$, the approximate primary diffusive 0'th order solution near $\tau=0$ is velocity $Wg_0(y,t)$ with non-dimensional deficit or interference $g= G- g_0$ such that

$$\mathbf{d}_t\, g - \mathbf{d}^2{}_y g = D[g]=0 \quad g=G(t) \text{ at } y=0 \quad (4)$$

Now the pressure gradient due to the acceleration of the coreflow parallel to the wall $\mathbf{d}_X p = -\rho\, G^2 W\mathbf{d}_X W$ will perturb this boundary layer more than the correction for the acceleration in the boundary layer $\rho\, w\mathbf{d}_X w$ so the net "planar/pressure" 1'st order correction is $TW\mathbf{d}_X W\mathbf{v}_1$ where $T\mathbf{d}_X W<<1$

$$D[\mathbf{v}_1] = G^2 - g_0{}^2 = 2Gg - g^2 \quad (5)$$

The first term dominates and the net peaks at G^2 at the wall which of course restrains the response. Thus very strong shear is to be expected from it as of interest in atherogenesis. For instance, if the duct is also curved with centerline radius R as in Fig 1, the inviscid flow has a lateral centripetal pressure gradient $\mathbf{d}_Z p = -\rho G^2 W^2/R$ so that in the boundary layer a secondary lateral flow of $\mathbf{v}= T W^2 \mathbf{v}_1 /R$ starts towards the center of curvature.

For a longitudinal acceleration the walls are converging towards the center axis flow but the normal component u must decline to nil at the wall ie from (3) $u= -\mathbf{d}_X W\int_0^Y g_0 \, dY$ which increases at first as the square of the

distance from the wall where g_o=0 until linearly outside the boundary layer. So there is also a positive 1'st order correction to g_0 for – $u\mathbf{d}_Y w$ "advection in" or "indraft" as $TW\mathbf{d}_X W\, w_1$

where $D[w_1]= \mathbf{d}_Y g_o \int_0^Y g_o \mathrm{d}Y = \mathbf{d}_y g_o \int_0^y g_o \mathrm{d}y$ (6)

For a typical (starting) boundary layer profile such as g_o= Gerf η, $\mathbf{d}_\eta g_o \int_0^\eta g_o\, \mathrm{d}\eta$ peaks at about $G^2/10$ at $\eta \approx 1$ (where $2Gg\text{-}g^2 \approx .3$) before vanishing at infinity outside the boundary layer. So the w_1 response to this forcing can be expected to be about .1 v_1's and this is indeed borne out for the shear perturbations in both starting and oscillating coreflows. But anticipating section IV, comparing η moments about the boundary for the same G, the factor is about .3. Now

$\int_0^y g_o\, \mathrm{d}y = \int_0^y(G\text{-}g)\mathrm{d}y= \{yG\text{-}\int_0^y g\mathrm{d}y\}$ so $D[w_1]= \mathbf{d}_y g\, \{\text{-}yG+\int_0^y g\mathbf{d}y\}$ (7)

where the first term is the inviscid inflow dominating away from the wall, though near the wall it is cancelled to leave the net y^2 increase. So then the first order longitudinal acceleration correction terms to w are $TW\mathbf{d}_X W$ (v_1+w_1), small vs W as assumed if $T\mathbf{d}_X W<< 1.$

     Thus there are two basic and very different perturbed diffusion equations to be solved in all first order perturbations of a time diffusive boundary layer for spatial acceleration effects. Previously w_1+v_1 longitudinal or v_1 transverse have been laboriously solved for specific $G(t)$ eg impulsive, linear and quadratic or at $t= \infty$ harmonic [4] without interconnection or comparative understanding. Here general (particular) solutions for the w_1 and v_1 are presented and then the complete solutions found for any series in $\sqrt{t}$, and asymptotic solutions for a simple harmonic.

III.   Perturbation Solutions for General Time Variation

Since D is a linear differential operator with homogeneous solution g: $D[g]$=0 , then dg or $\mathbf{d}_y g$ are further solutions $D[\mathbf{d}g]$=0 and $D[\mathbf{d}_y g]$=0. Likewise the indefinite integral in t generates a solution, or the definite integral $\int_c^t g\mathbf{d}t$ if g=0 at $t=c$, and $\int_c^y g\mathbf{d}y$ if $g=\mathbf{d}_y g$=0 at $y=c$.   To generalize the inversion $e^{\text{-}ry}\int_c^y e^{\text{-}ry}g\mathbf{d}y$ of the basic differential factor $\mathbf{d}_y+r$ commutes with D provided $e^{\text{-}ry}g$ & $e^{\text{-}ry}\mathbf{d}_y g$ vanish at $y=c$. (This provides one way of generating the g for harmonic $G(t)$ starting at t=0 in section IV).

To find particular solutions of the above perturbed diffusion problems, simply note that $D[gE(t)]=g\mathbf{d}_tE$ and that if h is another homogeneous $D[h]=0$ solution, then $D[gh]=\text{-}2\, \mathbf{d}_y g\, \mathbf{d}_y h$ These immediately provide a particular solution to the simpler pressure problem $v_1= v_{1p} - v_{1h}$ the difference of particular and homogeneous parts such that

$$D[v_{1h}]=0\quad D[v_{1p}]=2Gg\text{-}g^2\quad v_{1p}=2g\int_0^t G\mathbf{d}t + \tfrac{1}{2}[\textstyle\int_\infty^y g\mathbf{d}y]^2\quad (8)$$

Then at y=0, $v_{1p}=v_{1h}=2G\int_0^t G\mathbf{d}t+\tfrac{1}{2}[\int_\infty^o g\mathbf{d}y]^2$ (9)   and $\mathbf{d}_y v_{1p}=2\mathbf{d}_y g\int_0^t G\mathbf{d}t\ \text{-}G\int_0^\infty g\mathbf{d}y$ (10)

For w_1 (7): $D[w_{1p}]=\mathbf{d}_y g\, \{\text{-}yG+\int_0^y g\mathbf{d}y\}$

Trying $\text{-}y\, \mathbf{d}_y g\int_0^t G\mathbf{d}t$ gives the dominant first term plus $2\mathbf{d}^2{}_y g\int_0^t G\mathbf{d}t$ or $2\mathbf{d}_t g\int_0^t G\mathbf{d}t$ which like the last term $\mathbf{d}_y g\int_0^y g\mathbf{d}y\} = \mathbf{d}_y g\, \{\int_0^\infty g\mathbf{d}y+\int_\infty^y g\mathbf{d}y\}$ is easily solved by the above properties to get

$$w_{1p}= \text{-}y\, \mathbf{d}_y g\int_0^t G\mathbf{d}t\ \ \text{-}2\mathbf{d}_t g\int_0^t \mathbf{d}t\int_0^t G\mathbf{d}t\ \ +\mathbf{d}_y g\int_0^t\int_0^\infty g\mathbf{d}y\ -\ \tfrac{1}{2}\,g\int_\infty^y\int_\infty^y g\mathbf{d}y\ \ (11)$$

at y=0 $w_{1p}=w_{1h}$ = $\text{-}2\mathbf{d}_t G\int_0^t \mathbf{d}t\int_0^t G\mathbf{d}t\ \ +\mathbf{d}_y g\int_0^t\int_0^\infty g\mathbf{d}y\ -\ \tfrac{1}{2}\,G\int_\infty^0\int_\infty^y g\mathbf{d}y\quad\quad D[w_{1h}]=0\ \ (12)$

$\mathbf{d}_y w_{1p}= \text{-}\mathbf{d}_y g\int_0^t G\mathbf{d}t\ \ \text{-}2\mathbf{d}^2{}_{t\,y} g\int_0^t \mathbf{d}t\int_0^t G\mathbf{d}t\ \ +\mathbf{d}_t G\int_0^t\int_0^\infty g\mathbf{d}y\ -\ \tfrac{1}{2}\,\mathbf{d}_y g\int_\infty^0\int_\infty^0 g\mathbf{d}y\text{-}\ \tfrac{1}{2}\,G\int_\infty^0 g\mathbf{d}y\ \ (13)$

 there are no common elements to v_{1p} and w_{1p} (because their fluid dynamic origins are distinct) so they are the simplest basis functions to solve versus any linear combination such as $v_{1p}+ w_{1p}$

IV.   Diffusive and Perturbation Solutions for Root Powers of Time

From the fundamental solution Q_0=erfc η of the diffusion equation $D[Q_0]$=0, where the diffusive similarity variable η=$\tfrac{1}{2}y/\sqrt{t}$, the same $\mathbf{d}_y$ and $\int_\infty^y \mathbf{d}y$ operators can construct series of solutions Q_n for $g=G(t) =\sqrt{t}^{\,n}$ at y=0 as in Table 1.

TABLE 1 $D[F_n]=0$ solved by Q_n and P_n of form $F_n =\sqrt{t}^{\,n}f_n(\eta)$ $F_n =d_y F_{n+1}$ $\eta=\tfrac{1}{2}y/\sqrt{t}$

With q and p both solving $f(\eta)$ such that $f_n=\tfrac{1}{2}f\,'_{n+1}$ $nf_n-\eta f_n\,'-\tfrac{1}{2}f_n\,''=0$

so $\tfrac{1}{2}nf_n= \eta f_{n-1}+f_{n-2}$ Define $\gamma_n =\Gamma[n+\tfrac{1}{2}]$

n	$\sqrt{t}^{\,n}$	$q_n(\eta)$	$q_n(0)=(-1)^n/\gamma_n$	$p_n(0)$	$p_n(\eta)= \tfrac{1}{2}\lim q_n(\eta)$ $\eta\Upsilon\text{-}\infty$
4	t^2	$16i_4\mathrm{erfc}(\eta)$	$\tfrac{1}{2}$	$\tfrac{1}{2}$	$\tfrac{1}{2} +2\eta^2+ 2\eta^4/3$
3	$\sqrt{t}^{\,3}$	$-8i_3\mathrm{erfc}(\eta)$	$-4/3\sqrt{\pi}$	0	$2\eta+4\eta^3/3$
2	t	$4i_2\mathrm{erfc}(\eta)$	1	1	$2\eta^2+1$
1	$\sqrt{t}$	$-2i_1\mathrm{erfc}(\eta)$	$-2/\sqrt{\pi}$	0	2η
0	1	$\mathrm{erfc}(\eta)$	1	1	1
-1	$1/\sqrt{t}$	$-e^{-\eta^2}/\sqrt{\pi}$	$-1/\sqrt{\pi}$	0	$2e^{-\eta^2}\int_0^\eta e^{z^2}dz =p_{-1}$
-2	t^{-1}	$\eta e^{-\eta^2}/\sqrt{\pi}$	0	1	$1-\eta\, p_{-1}$
-3	$t^{-3/2}$	$(\tfrac{1}{2}-\eta^2)e^{-\eta^2}/\sqrt{\pi}$	$\tfrac{1}{2}\,/\sqrt{\pi}$	0	$(\eta^2-\tfrac{1}{2})\, p_{-1} -\eta$
-4	t^{-2}	$(\eta^3-3\eta/2\,)e^{-\eta^2}/\sqrt{\pi}$	0	-1	$(-\eta^3+3\eta/2)\, p_{-1}+ (\eta^2-1)$

Notes: The multiplier of $-e^{-\eta^2}/\sqrt{\pi}$ is the same as the multiplier of $p_{-1}= 2\mathrm{DawsonF}(\eta)$ The negative index $P_{-n}= d^{n-1}{}_y$ ($2\mathrm{DawsonF}(\eta)/\sqrt{t})$ so $p_{-n}= (\tfrac{1}{2})^{n-2} d_\eta{}^{n-1}\mathrm{DawsonF}(\eta)$ which alternates in non-zero value at $y=\eta=0$ with the q_{-n} to allow solution for $G(t)$ as asymptotic series in inverse powers of large time. The p_n series breaks between $\int_\infty^y p_{-1}dy$ divergent and $d_y p_0=0$, and for positive index the p_n diverge at infinity.

_____

These solutions of the general form $F_n=\sqrt{t}^{\,n}f_n(\eta)$ so $d_y =d_\eta / 2\sqrt{t}$ $dy=2\sqrt{t}\, d\eta$.

$D= \partial_t -\tfrac{1}{2}\eta\, t^{-1}\partial_\eta - \tfrac{1}{4}t^{-1}\partial^2_\eta$ so $D[F_j] =\tfrac{1}{2}\sqrt{t}^{\,n-2}(nf_n-\eta f_n\,'-\tfrac{1}{2}f_n\,'') =0$

a second order ode with two independent set of solutions being the $Q_n=\sqrt{t}^{\,n}q_n(\eta)$ and $P_n=\sqrt{t}^{\,n}p_n(\eta)$ tabulated above. Since all $f_n(\eta)$ are series of η derivatives, this o.d.e gives the recursion relation…… $\tfrac{1}{2}nf_n= \eta f_{n-1}+f_{n-2}$ useful for computing.

For non-negative n, $q_n =(-2)^n i_n\mathrm{erfc}(\eta)=(-2)^n i_n$ the iterated complementary error functions as in Figure 2 where $d_\eta i_n= -i_{n-1}$. All q_n or i_n vanish at infinite η.

So for $G(t) = \Sigma\, a_n\sqrt{t}^{\,n}$ (with $\int_0^t G dt= \Sigma\, 2a_n\sqrt{t}^{\,n+2}/ n+2)$ $g= \Sigma\, a_n\gamma_n (2\sqrt{t})^n i_n$ where the $\gamma_n= \Gamma(\tfrac{1}{2}n+1)$

normalize the $2^n i_n$ as in Figure 2. Note $\gamma_n/ \gamma_{n-2} = \tfrac{1}{2}n$.

Remember $i_{n+1}=\int_\eta^\infty d_\eta\, i_n$ so the primary shear is $d_y g= -\Sigma a_n\gamma_n (2\sqrt{t})^{n-1}i_{n-1}$. Thus with a pulsatile flow for example a parabolic pulse, the shear reverses before the coreflow. Then from (8) and (9)

$$v_1=\Sigma\Sigma\, a_n a_s(2\sqrt{t})^{n+s+2}[\gamma_n i_n/2^s(s+2)+ \tfrac{1}{2}\gamma_n i_{n+1}\gamma_s i_{s+1} -\gamma_{n+s+2}\, i_{n+s+2}\{4/(s+2)+ \tfrac{1}{2}\gamma_n\gamma_s/\, \gamma_{n+1}\gamma_{s+1}\}] \quad (14)$$

As anticipated the v_{1p} or first two terms in the bracket are positive with negative shear reflecting the increase of the forcing towards the boundary. So the positive shear of the negative $\{\}$homogeneous solution must prevail, since the overall shear should be positive. Physically the strong slip of the particular solution at the boundary from the forcing generates strong homogeneous shear, dominating the weak reverse shear from the decrease of the particular solution away from the boundary. So from (10) and (14)

at $y=0$ $d_y v_1=\Sigma\Sigma a_n a_s(\sqrt{t})^{n+s+1}[-4\gamma_n/\, \gamma_{n-1}(s+2) - \gamma_n/\gamma_{n+1}+\gamma_{n+s+2}/\, \gamma_{n+s+1}\{4/(s+2)+\tfrac{1}{2}\gamma_n\gamma_s/\, \gamma_{n+1}\gamma_{s+1}\}] \quad (15)$
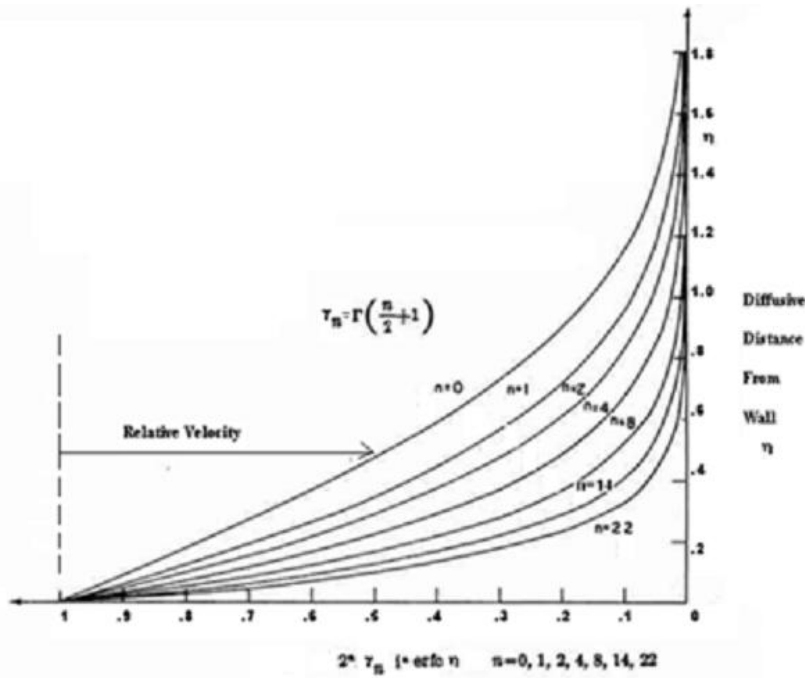
Figure 2   Repeated Integrals of the complementary error function

Comparing the two particular wall shears for $n=s$, $4\gamma_{n+1}/\gamma_{n-1}=2(n+1)$ vs. $(n+2)$ so the first particular term dominates with increasing n from equality at $n=0$. Regarding Figure 2 as relative velocity profiles it is clear that the shear of the homongeneous normalised i_{2n+2} dominates the first particular and so the sum even though it is less than the shear of the square of i_{n+1} in the second terms.

Evaluating the w_1 perturbation requires further

$\int_y^\infty g\,dy = \Sigma a_n\gamma_n (2\sqrt{t})^{n+1}i_{n+1}$ $\mathbf{d}_\eta g = -\Sigma a_n\gamma_n(2\sqrt{t})^n i_{n-1}$, $\mathbf{d}_t G = \Sigma \frac{1}{2} na_n\sqrt{t}^{\,n-1}$,

$\int_0^t\int_0^t G\,dt = \Sigma 4a_n\sqrt{t}^{\,n+4}/(n+2)(n+4)$, $\int_0^t g = \int_\infty^y\int_\infty^y g\,dy = \Sigma\ a_n\gamma_n (2\sqrt{t})^{n+2}i_{n+2}$, $\mathbf{d}_t g = \mathbf{d}^2_y g = \Sigma a_n\gamma_n (2\sqrt{t})^{n-2}i_{n-2}$,

$\mathbf{d}^2_{ty} g = \mathbf{d}^3_y g = -\Sigma a_n\gamma_n (2\sqrt{t})^{n-3}i_{n-3}$, $\int_0^t\int_0^\infty g\,dy = \Sigma 2a_n\gamma_n (\sqrt{t})^{n+3}/\gamma_{n+1}/n+3$,

$\int_\infty^y\int_\infty^y g\,dy = \Sigma a_n\gamma_n (2\sqrt{t})^{n+2}i_{n+2}$ $\int_\infty^0\int_\infty^0 g\,dy = \Sigma 2a_n (2\sqrt{t})^{n+2}/n+2$

so that

$$w_{1p} = \Sigma\Sigma\ a_n a_s(\sqrt{t})^{n+s+2}[\eta 2^{n+1}\gamma_n i_{n-1}/(s+2)-2^{n+1}\gamma_n i_{n-2}/(s+2)(s+4)-2^n\gamma_n i_{n-1}\gamma_s/\gamma_{s+1}(s+3)-2^{n+s+1}\gamma_s i_s\gamma_n i_{n+2}] \quad (16)$$

The first term dominant at average η vanishes at the boundary leaving the negative corrections terms with positive shear. But the positive shear of the dominant term means the negative shear of the positive homogeneous terms is overcome. $w_1 = w_{1p} - w_{1h}$ Here the wall shear is dominated by the particular solution increasing with distance from the boundary like the forcing just overcoming the weak homogeneous shear from the weak slip of the particular solution , the opposite situation from v_1.

$$w_{1p} = w_{1h} = \ \Sigma\Sigma\ a_n a_s\sqrt{t}^{\,n+s+2}[\ -4n/(s+2)(s+4) -2\gamma_n\gamma_s/\gamma_{n-1}\gamma_s (s+3) -\tfrac{1}{2}\gamma_n/\gamma_{n+2}] \quad \text{at } y=0 \quad (17)$$

$$w_{1h} = \ -\Sigma\Sigma\ a_n a_s(2\sqrt{t})^{n+s+2}[4n/(s+2)(s+4)+2\gamma_n\gamma_s/\gamma_{n-1}\gamma_{s+1}(s+3)+1/n+2]\gamma_{n+s+2}\,i_{n+s+2} \quad (18)$$

At $y=0$ $\qquad\qquad \mathbf{d}_y w_{1h} = \Sigma\ \Sigma a_n a_s(2\sqrt{t})^{n+s+1}[\qquad " \qquad\qquad\qquad\qquad " \qquad]\gamma_{n+s+2}/\gamma_{n+s+2} \quad (19)$

$$\mathbf{d}_y w_{1p} = \Sigma\Sigma a_n a_s\sqrt{t}^{\,n+s+1}[2\gamma_n/\gamma_{n-1}(s+2)+8\gamma_n/\gamma_{n-3}/(s+2)(s+4)+n\gamma_s/\gamma_{s+1}/(s+3)+\gamma_n/\gamma_{n-1}/(s+2)+\tfrac{1}{2}\gamma_n/\gamma_{n+1}] \quad (20)$$

This has a very high degree of reduction by the homogenous shear so the net positive shear is as expected about $1/10^{th}$ of $\mathbf{v_1}$'s declining similarly with $\boldsymbol{n}$. So in the combined axial acceleration problem $\mathbf{v_1}$ will totally dominate the shear, as anticipated due to the $\boldsymbol{w_1}$ forcing peaking low in the middle of the primary boundary layer.

The aortic systolic flow pulse was represented by a quartic polynomial in $\boldsymbol{t}$ by and the above diffusion approach was extended to higher order and to the aorta entry by beginning diffusion at the $t{\geq}0$ when the Oseen .35 times the inviscid flow left this leading edge of the wall. The 2 first order perturbation and the linear $\boldsymbol{\tau}$ terms then agreed to +/- 20% with perturbations of the Blasius solution. [1]

But the sharp curvature in the aortic arch makes the $\mathbf{v_1}$ and higher secondary flow perturbations very strong, indeed too strong at the inside of the strongest bend where the secondary flows converge to a stagnation point, and so thicken the boundary layer that it separates. Actually this begins just downstream of the maximum bend where the axial coreflow is also decelerating longitudinally on the inside of the bend. The separation of the boundary layer in the computations was seen in ultrasound measurements in humans by Perroneau[3].

V.   Stokes Transformation, Layer, and Steady Streaming

The Stokes 'layer' $S= e^{rt+y\sqrt{r}}$, $\mathbf{d}_y S=S\sqrt{r}$ $D[S]=0$ solves the diffusion equation with complex $\sqrt{r}$

If any solution at all D[$\boldsymbol{Q}$]=0 is expressed in terms of $\boldsymbol{t}$ and $\boldsymbol{\eta}$ ie as $\boldsymbol{Q(t,\eta)}$ and ' again denotes differentiation wrt the second (similarity) variable $\eta=\frac{1}{2}y/\sqrt{t}$

$\partial_t Q-\frac{1}{2}\eta Q'/t-\frac{1}{4}Q''/t=0$ again. Now if $\zeta=\eta+\sqrt{rt}$ then $d_t\zeta=-\eta/t+\frac{1}{2}\sqrt{r/t}=-\zeta/2t+\sqrt{r/t}$ so

$D[SQ(t,\zeta)]=D[S]Q+SD[Q]-2\mathbf{d}_yS\mathbf{d}_yQ=S\{\partial_tQ-\frac{1}{2}\zeta\,Q'/t-\frac{1}{4}Q''/t)+Q'\sqrt{r/t}\,\}-2rSQ'\mathbf{d}_y\eta=SQ'\sqrt{r/t}-2SQ'\frac{1}{2}\sqrt{r/t}=0$

So "Stokes transforming" any solution $\boldsymbol{Q(t,\eta)}$ may give one other solution $\boldsymbol{Q_{\sqrt{r}}=S\,Q(t,\eta+\sqrt{rt})}$. Transforming again at -$\sqrt{r}$ reverts to the original $\boldsymbol{Q(t,\eta)}$ or at $\sqrt{r}$ just transforms once at $2\sqrt{r}$. Since $(\eta+\sqrt{rt})^2=\eta^2+y\sqrt{r}+rt$, $\boldsymbol{S}$exp $-(\eta+\sqrt{rt})^2=$ exp$-\eta^2$, the $\boldsymbol{Q_j}$ of negative index aren't changed [1] but for all the $\boldsymbol{Q_n}$ of positive index $\boldsymbol{Q_{n,\sqrt{r}}=e^{rt+y\sqrt{r}}(2\sqrt{t})^n\mathbf{i}_n\mathbf{erfc}(\eta+\sqrt{rt})}$ are distinct solutions. A less general, more arduous construction is $\boldsymbol{Q_{n,\sqrt{r}}=e^{y\sqrt{r}}\int_{\infty}^{y}e^{-y\sqrt{r}}\,Q_{n-1,\sqrt{r}}\,\mathbf{dy}}$

Note $\mathbf{erfc}(z) + \mathbf{erfc}(-z) =2$ so the solution for $\boldsymbol{G}(t)= \mathbf{e}^{rt}$ complex exponential starting at $t{=}0$ is [2]

$\boldsymbol{g}=\frac{1}{2}(\boldsymbol{Q_{0,\sqrt{r}}} +\boldsymbol{Q_{0,-\sqrt{r}}})= \frac{1}{2}\mathbf{e}^{rt}\{\mathbf{e}^{y\sqrt{r}}\mathbf{erfc}(\eta+\sqrt{rt})+ \mathbf{e}^{-y\sqrt{r}}\mathbf{erfc}(\eta-\sqrt{rt})\}$. (21)

$\boldsymbol{y}$ integrations of $\boldsymbol{Q_{0,\sqrt{r}}}=e^{y\sqrt{r}}\int_{\infty}^{y}\mathbf{dy}\,e^{-y\sqrt{r}}\,e^{-\eta^2}/\sqrt{\pi t}$ for the particular solutions are possible by parts.

Eg. $\int_{\infty}^{y}\boldsymbol{g}\mathbf{dy}=\frac{1}{2}(\boldsymbol{Q_{0,\sqrt{r}}} -\boldsymbol{Q_{0,-\sqrt{r}}})/\sqrt{r}$, $\int_{\infty}^{y}\int_{\infty}^{y}\boldsymbol{g}\mathbf{dy}=\frac{1}{2}(\boldsymbol{Q_{0,\sqrt{r}}} +\boldsymbol{Q_{0,-\sqrt{r}}})/r+ \boldsymbol{Q_0}/\sqrt{r}$

So $\int_{\infty}^{0}\boldsymbol{g}\mathbf{dy}= \mathbf{e}^{rt}\,\mathbf{erf}\,(\sqrt{rt})/\sqrt{r}$ as in Fig 3 but upon squaring this has defeated exact homogeneous solution $\mathbf{v_{1h}}$. But asymptotic ones will be considered after clarifying the asymptotics of $\boldsymbol{g}$ and how real $\boldsymbol{g}$ relates to the complex. For large $|rt|>>\eta$ or $t >> \frac{1}{2}y/|r|$ $\mathbf{erfc}(z)\approx e^{-z^2}/z\sqrt{\pi}$ $(1-\frac{1}{2}/z^2+..)$ for large z [5] . Then

$$\boldsymbol{g}\approx \mathbf{e}^{rt-\sqrt{r}\,y} - \boldsymbol{Q_{-2}}/r - \boldsymbol{Q_{-4}}/r^2+\ldots(22)$$

where the second term as $\boldsymbol{t}^{-1}$ will asymptotically dominate for all $\boldsymbol{r}$ with a negative real part. As $\boldsymbol{Q_{-2}}=\mathbf{d}_t \boldsymbol{Q_0} = \mathbf{d}_t\mathbf{erfc}\eta$ it represents the languishing as $\boldsymbol{t}^{-1}$ at diffusing distance η of some effective net $\boldsymbol{g}$ from small $\boldsymbol{t}$. For positive real part of $\boldsymbol{r^2}$ or exponential growth $\boldsymbol{g} \approx S\approx \mathbf{e}^{rt-y\sqrt{r}}$ the Stokes layer has an oscillatory component in $\boldsymbol{y}$ if $\boldsymbol{G}$ has one in $\boldsymbol{t}$. For pure oscillatory imaginary $\boldsymbol{r}$ at $\boldsymbol{k}$'th harmonic $r=ik$. Choosing and henceforth implying the Real part by a $\mathbf{cos}\,t$ (impulsive) start avoids the imaginary $\boldsymbol{Q_{-2}}/r$ so the correction is - $\boldsymbol{Q_{-4}}/r^2$ as $\boldsymbol{t}^{-2}$ which doesn't complicate the study of the asymptote to steady streaming. Then at large $\boldsymbol{t}$

$$\boldsymbol{g}\approx\mathbf{e}^{it-y\sqrt{i}} +\boldsymbol{Q_{-4}}\approx\mathbf{e}^{-y/\sqrt{2}}\mathbf{cos}(t-y/\sqrt{2})+\boldsymbol{Q_{-4}},\ \ \mathbf{d}_y\boldsymbol{g}=-\mathbf{e}^{-y/\sqrt{2}}\mathbf{cos}(t-y/\sqrt{2}+\frac{1}{4}\pi)+\boldsymbol{Q_{-5}},\ \int_{\infty}^{0}\boldsymbol{g}\mathbf{dy}\approx-\mathbf{cos}(t-\frac{1}{4}\pi)+\boldsymbol{Q_{-3}}\ \ (23)$$

[1] though transforming Dawson's integral solves the unbounded $\boldsymbol{G}(t)= \boldsymbol{i}\,t^{-\frac{1}{2}}\mathbf{erf}\,\boldsymbol{i}\sqrt{rt}$.

[2] Recursion gives $\mathbf{i_1}\mathbf{erfc}(z)= -z\mathbf{erfc}(z)+ \boldsymbol{Q_{-1}}$ so even in z $\boldsymbol{g}= (\mathbf{Q_{1,-r}}- \mathbf{Q_{1,r}})/\,4\sqrt{r}$ solves $\boldsymbol{G}(t)= t\mathbf{e}^{rt}$ from $t{=}0$

As in Fig 3 the transient between $\int_\infty^0 g\,dy = \mathbf{Re\{-e^{it}\,erf\sqrt{it})/\sqrt{i}\}}$ and $\mathbf{-cos}(t\mathbf{-\tfrac14\pi})$ can alternatively be uniformly approximated by the sum of two exponential decays $\mathbf{.18e^{-.4t}+.5e^{-4t}}$. The square of this accurate $\int_\infty^0 \mathbf{g\,dy}$ would give $\mathbf{v_{1h}}$ at y=0 in complex exponentials again, which can be solved
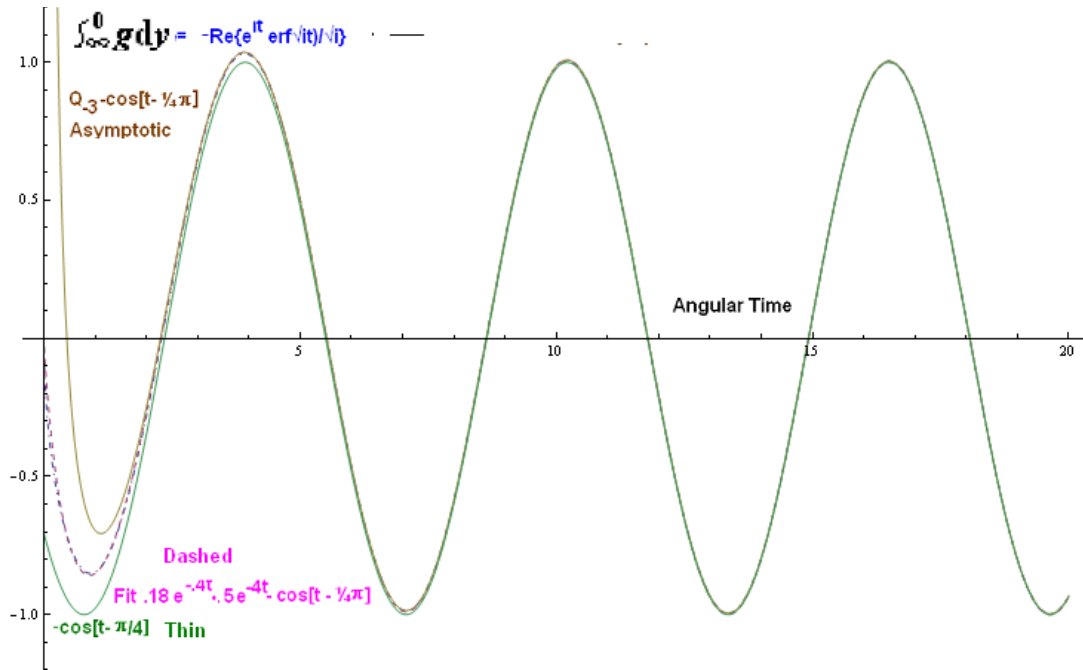
Figure 3 Approximations to the y integral of g for $G= \cos t$ from t=0

by the above with complex r. Including these decays would give small corrections to the following coefficients of Q_{-2} or t^{-1} asymptotes which arise entirely in the homogeneous problems**.**   With the asymptotic g, the solution $\mathbf{v_1}$ is straightforward to determine

$$\mathbf{v_1 \approx 2\ e^{-y/\sqrt2}cos(t-y/\sqrt2)\ sin}t + \tfrac12\,\mathbf{e^{-y\sqrt2}\ cos^2(}t\mathbf{-y/\sqrt2- \tfrac14\pi)\ -5e^{-y}sin(2}t\mathbf{-y)/8 - \tfrac14\ erfc}\eta\ \mathbf{-5Q_{-2}/8}\quad(23)$$

The square of the y integral of the primary Stokes oscillation in y and t thus creates a mean particular flow at the wall whose homogeneous reaction diffuses to infinity as a $\mathbf{Q_0=erfc}\eta$. The second harmonic homogeneous terms carries a $\mathbf{Q_{-2}}$ or t^{-1} correction from (21). Because the particular solutions asymptote faster as t^{-2} there is no point in using the exact ones, but those do show the asymptotic particular solutions below do not need to be corrected for initial values. From (10) and (23)

$$\mathbf{d_y v_1 \approx \tfrac14 \sqrt2 +(5/4\sqrt2 -3/2)sin(2}t\mathbf{+\tfrac14\pi) -\tfrac14 Q_{-1} -\tfrac58 Q_{-3} \approx .353 +.267sin(2}t\mathbf{+\tfrac14\pi) +\tfrac14/\ \sqrt{}t\pi\ -5/\ 16\sqrt{}\pi t^3}\quad(24)$$

So the mean wall shear decays as $\mathbf{1/\sqrt{}}t$ to an ultimate positive wall shear of mean $\mathbf{\tfrac14\sqrt2}$ with second harmonic. Thus the forcing in the Stokes layer is met by a particular solution confined to the Stokes layer but slipping at the wall. That generates vorticity / a homogeneous solution to prevent slip whose mean diffuses and spreads all the way out to the outer flow in time.

The mean shear is just the time average of the y integral of the forcing, whilst as eqn 5.13.19 [4] the streaming mean velocity is the time average of the y moment of the forcing. Now the $\mathbf{v_1}$ forcing is strong and near the wall whilst the $\mathbf{w_1}$ forcing is weak but further from the wall so its streaming mean velocity can be much more significant than its shear.

 The constant values in (11) at t=0 multiply homogeneous solutions, so these are exactly cancelled by their counterparts in w_{1h}, and all that briefly survives are the t^{-1} asymptotes due to these initial values. (This did not arise in the power of $\sqrt{}t$ basis as all t integrations are automatically zero at t=0.)

The highest error term in w_{1p} comes from the highest integrated term $\int_0^t \int_0^\infty \mathbf{g\,dy}$ of $\mathbf{Q_{-1}}$ multiplying $\mathbf{d_y\,g}$ to give a term at the wall as $\cos(t\mathbf{- \tfrac14\pi})/\sqrt{}\pi t$ whose homogeneous solution is unfortunately unknown. How the running mean of this boundary value decays should be how its mean diffused value would decay. The running

total is $\int^t \cos(t+\tfrac{1}{4}\pi)/\sqrt{t}$ = (FresnelS-FresnelC)$\sqrt{2}\sqrt{t}$ which tends to 0 so there is no mean transient $1/t$ response to add to those from the homogeneous pure harmonics (that do not start as cos's). So then

$w_{1p} \approx ye^{-y/\sqrt{2}}\cos(t-y/\sqrt{2}+\tfrac{1}{4}\pi)\sin t - 2e^{-y/\sqrt{2}}\sin(t-y/\sqrt{2})\cos t - \tfrac{1}{2}e^{-y\sqrt{2}}\sin(2t-y/\sqrt{2}) + \tfrac{1}{2}e^{-y\sqrt{2}}\cos(y/\sqrt{2}) - \tfrac{1}{4}e^{-y\sqrt{2}}\sin(2t-\sqrt{2}y)$

$w_{1h} = -7e^{-y}\sin(2t-y)/4 + \tfrac{1}{2}\,\mathbf{erfc}\,\eta + 13Q_{-1}/8$ (26)

Here the mean of w_{1p}'s $\mathbf{d}_y g \int_0^t \int_0^\infty g dy'$ is twice as strong at $y=0$ as the mean of $\mathbf{v}_1$'s <u>half</u> square $\tfrac{1}{2}[\int_\infty^y g dy]^2$. Thus each wall mean just comes from one in-phase "square" term, and w_{1p}'s is clearly if suprisingly twice as strong as $\mathbf{v}_{1p}$'s. Equation (13) is more direct than (26) for some of the shear terms.

$$\mathbf{d}_y w_1 \approx (5/2 - 7\sqrt{2}/4)\sin(2t+\tfrac{1}{4}\pi) - \tfrac{1}{2}Q_{-1} - 13Q_{-3}/8 \approx +.025\sin(2t+\tfrac{1}{4}\pi) + \tfrac{1}{2}/\sqrt{t\pi} - 13/\,16\sqrt{\pi t^3} \quad (27)$$

The second harmonic component is about $1/10^{th}$ of $\mathbf{v}_1$'s, as expected from section I. Three terms in w_{1p}, have ultimate mean shears but they cancel. Thus the ultimate mean w_1 flux into the $y=0$ sink vanishes so there is no net mean w_{1p} forcing integrated over y. The higher steady w_1 streaming comes from more of the mean w_1 produced further from the wall sink than $\mathbf{v}_1$ diffusing to infinity. The w_1 mean forcing from $-\mathbf{d}_y g \int_0 g dy\}$ decays as $e^{-y\sqrt{i}}$ whereas the $\mathbf{v}_1$ mean forcing from $-g^2$ decays as $e^{-y\sqrt{2}}$ so the former has twice the y moment and so twice the steady streaming. [3]

$$\mathbf{d}_y(\mathbf{v}_1 + w_1) \approx .353 + .292\sin(2t+\tfrac{1}{4}\pi) + \tfrac{3}{4}/\sqrt{t}\,\pi - 9/8\sqrt{\pi t^3} \quad (28)$$
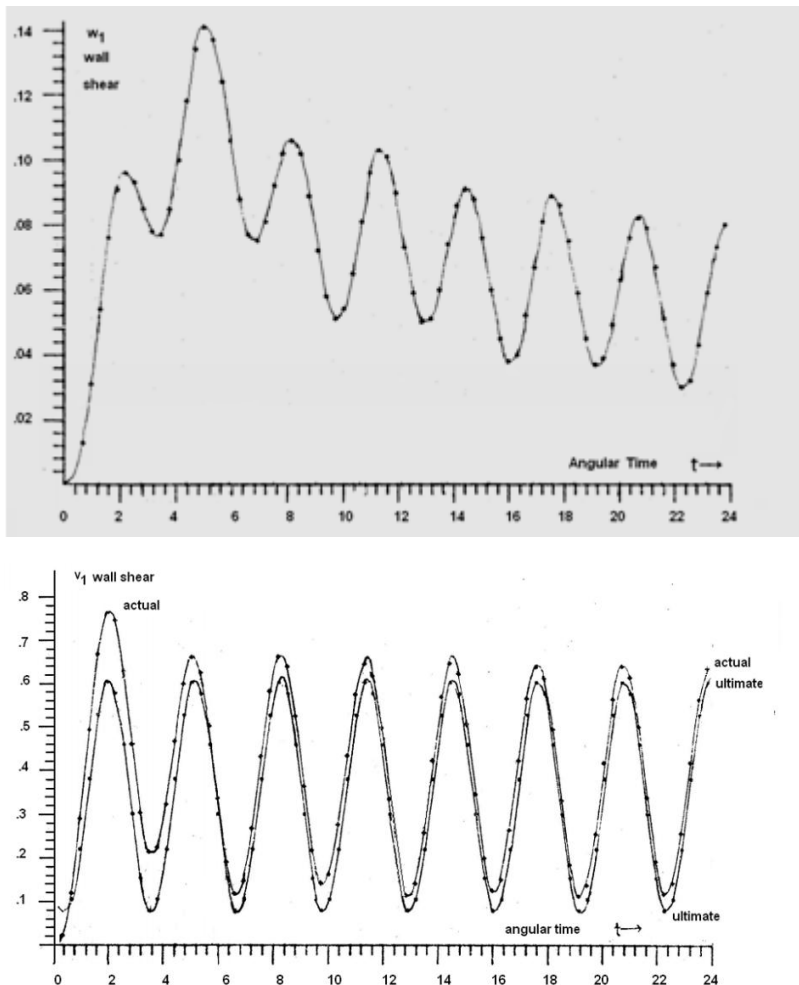

Figure 4 Perturbation wall shears computed for *G*=sin *t* from *t*=0 by Taylor series. NB different shear scales.

[3] [4] twice attributes steady streaming under longitudinal acceleration to just the w_1 momentum transfer by mean $u\mathbf{d}_y w$ but calculates the net from $\mathbf{v}_1 + w_1$. Though a 50% enhanced w_1 is indeed solely responsible for the **phase** steady streaming in $-\tfrac{3}{4}WT(\mathbf{d}_X W + W\mathbf{d}_X\gamma)$ under a wave coreflow $W\mathbf{Re}\{e^{it+i\gamma}\}$ in Batchelor's (5.13.20).

The combined shear is practically $\mathbf{d_y v_1}$ except the transient shear from the outward diffusion of the steady streaming is trebled. In Taylor series calculations for *G*= **sin** *t* from *t*=0 convergence was accelerated by the Pade method[6,7] . Fig 4 shows the high steady streaming transient shear of w_1 declining slowly as $t^{-\frac{1}{2}}$ to the low ultimate second harmonic shear. The transient first harmonics in w_1 decline as t^{-2}. The large ultimate mean and second harmonic dominate the small steady streaming transient in $d_y v_1$.

VI.   Conclusions

The perturbation of a time-diffusive boundary layer for longitudinal acceleration is the sum of a pressure gradient perturbation large near the wall and a 'indraft' perturbation with a modest peak in the middle of the boundary layer. The first gives an order of magnitude greater shear, but the second has twice the steady streaming flow which spreads outwards as the complementary error function of the diffusive similarity variable. This gives twice the transient shear declining as the inverse square root of time. The next order transient outward diffusion is an inverse time function of the diffusive similarity variable. For moderate time, a Taylor series in time numerically converges for almost 5 cycles of a harmonic. For any such (root) time series, the general particular solutions found are easily matched with exact homogenous ones to complete an explicit exact perturbation solution.

References

[1]   Farthing S., Flow in the thoracic aorta and its relation to Atherogenesis Ph.D. thesis 1977 University of Cambridge, Cambridge England

[2]   Cunningham K.S., Gotlieb A.I. The role of shear stress in the pathogenesis of atherosclerosis.   Lab Invest. 2005 85(1):9-23

[3]   Perroneau , P. Flow in the thoracic aorta. Cardiovascular Research 1979 13 (11) 607-620

[4]   Batchelor, G.K. (1970) An Introduction to Fluid Dynamics Cambridge Univ. Press p.358

[5]   Abramowitz, M.; Stegun, I. A., eds. *Handbook of Mathematical Functions with Formulas, Graphs, and Mathematical Tables*, New York: Dover Publications1972,

[6]   Shanks, D. "Non-linear transformation of divergent and slowly convergent sequences", *Journal of Mathematics and Physics* 1955 **34**: 1–42

[7]   Wynn, P. "On a device for computing the $e_m(S_n)$ transformation". *Mathematical Tables and Aids of Computation* 1956 ***10***: 91–96.